OXFORD

Properties of carbon nanotube-dispersed Sr-hydroxyapatite injectable material for bone defects

M. G. Raucci[1,*], M. Alvarez-Perez[2], D. Giugliano[1], S. Zeppetelli[1] and L. Ambrosio[1,3]

[1]Institute of Polymers, Composites and Biomaterials, National Research Council of Italy, Mostra D'oltremare Pad.20 - Viale Kennedy 54, Naples 80125, Italy; [2]Tissue Bioengineering Laboratory, DEPeI, Faculty of Dentistry, National Autonomous University of Mexico, Mexico DF 04510, Mexico; [3]Department of Chemical Sciences and Materials Technology, National Research Council of Italy, (DSCTM-CNR), P.Le Aldo Moro 7, Rome 00185, Italy

*Correspondence address. IPCB-CNR - Mostra d'Oltremare Pad.20, Viale Kennedy 54 - 80125 Naples, Italy. Tel: +39 081 2425945; Fax: +39 081 2425932; E-mail: mariagrazia.raucci@cnr.it

Abstract

This study concerns the synthesis of gel materials based on carbon nanotubes dispersed strontium-modified hydroxyapatite (Sr-HA) at different compositions obtained by sol–gel technology and their influence on human-bone-marrow-derived mesenchymal stem cells. Furthermore, an evaluation of the influence of nanotubes and Strontium on physico-chemical, morphological, rheological and biological properties of hydroxyapatite gel was also performed. Morphological analysis (scanning electron microscopy) shows a homogeneous distribution of modified nanotubes in the ceramic matrix improving the bioactive properties of materials. The biological investigations proved that Sr-HA/carbon nanotube gel containing 0–20 mol (%) of Sr showed no toxic effect and promote the expression of early and late markers of osteogenic differentiation in cell culture performed in basal medium without osteogenic factors. Finally, the SrHA/carbon nanotube gels could have a good potential application as filler in bone repair and regeneration and may be used in the osteoporotic disease treatment.

Keywords: nanobiomaterials; sol-gel tecnology; biomaterial-cell interaction; bioceramics; bone tissue engineering

Introduction

Because of the aging of population, the requirement for new bone substitute is growing very rapidly in the last decade. As a result, there is a great request of bioceramics with detailed properties such as anti-inflammatory, antibacterial and/or anti-osteoporotic properties [1]. In this context, the developing of innovative biomaterials, it is required to take in consideration that they will be used in the treatment where the bone remodeling is compromised. It is known that Strontium (Sr) has an important role in the bone remodeling, operating with both the stimulation of bone formation and a reduction in bone resorption. In fact, Sr^{2+} ions show the capability not only to increase osteoblast-related gene expression and the alkaline phosphatase (ALP) activity of mesenchymal stem cells (MSCs), but also to constrain the differentiation of osteoclasts [2, 3]. *In vitro* and *in vivo* studies have demonstrated that an improvement of bone

formation through an increasing of the bone mineral density and a decreasing of bone resorption was obtained by an oral strontium intake [4]. Moreover, several studies have also reported that Sr is used for osteoporosis treatment, inducing osteoblast activity when complexed in biocompatible bone cements [5, 6].

As a result, it is assumed that Sr has an effective role to enhance the bioactivity and biocompatibility of biomaterials and, in particular, to have potential in the treatment of osteoporosis [7, 8]. However, calcium phosphate (CaP) materials show limited compressive strength and their uses are limited to non-stress-bearing applications as maxillofacial surgery, or the repair of craniofacial defects and dental fillings [9]. Several studies are focused to develop CaP composite materials with better mechanical performance by using reinforcement component. In this view, a variety of reinforcing elements as polymers (i.e. poly-ε-caprolactone, poly-L-lactide, etc.) and carbon nanotubes

(CNTs) can be considered [10, 11]. In fact, a great attention in the applications of CNTs is based on their use as reinforcement in different materials for their important mechanical properties [12–14]. CNTs are also studied for other biomedical applications such as neural implants and tissue scaffolds, using their high tensile strength, electrical conductivity and chemical stability [15, 16].

In this context, an important interest is the possibility to use composite materials containing CNTs for bone tissue engineering [17], because they show the potential to strengthen and toughen CaP without reducing its bioactive properties, thus expanding a range of clinical applications for the materials. Several researchers have used CNTs as an inorganic phase for development of novel CNT-based bone graft materials (HA-CNTs) to improve mechanical properties [18, 19] and bioactivity [20], respectively. This may be obtained for the good mechanical properties of CNTs and the bioactive properties of HA. Generally, the composite materials used as synthetic bone grafts should be osteoconductive to improving integration with the bone tissue in the body. On this basis, this research was conducted to investigate the synthesis of an injectable composite material based on hydroxyapatite containing strontium (Sr-HA) and CNTs as a reinforcing component. Conventional processes to produce HA-CNT composite materials are based on physicochemical blending methods including ball milling [21] and mixing in solvent [22]. This leads to an inhomogeneous distribution of the nanotubes in the ceramic phase reducing the bioactive properties of material. Here, we propose the development of Sr-containing hydroxyapatite bone cement reinforced by MWCNT (SrHA/CNT) by using a simple route like sol–gel technology to obtain a homogenous and bioactive composite materials.

Materials and Methods

Synthesis of CNT-doped Sr-hydroxyapatite gels
Gel materials containing 10, 15 and 20 mol% Ca^{2+} replaced by Sr^{2+} (SrHA/CNT) were synthesized at room temperature by sol–gel approach using calcium nitrate tetrahydrated $Ca(NO_3)_2 \cdot 4H_2O$ (Sigma-Aldrich, Italy) and di-phosphorous pentoxide P_2O_5 (Sigma-Aldrich, Italy) as precursors of hydroxyapatite. Strontium nitrate $(Sr(NO_3)_2$, Sigma-Aldrich, Italy) was dissolved in water and used to replace Ca^{2+} ions. A Ca + Sr aqueous solution was obtained to dissolving calcium nitrate tetrahydrated precursor in water at room temperature (Ca solution; 3M) following by adding of $Sr(NO_3)_2$ (3M) solution. After mixing for 60 min, a solution based on MWCNT-COOH (0.5%wt, Nanocyl) was added. Then, Phosphorous solution was introduced drop-wise to system in an appropriate amount to achieve a (Ca + Sr)/P ratio of about 1.67. The sodium dodecyl sulphate (0.5%wt SDS, Sigma-Aldrich) was used as a dispersant. The medium alkalinity was adjusted by addition of NH_4OH up to pH 10 to improve the crystalline grade of phase. The systems at different composition were sonicated for 2 h followed by an aging step of 2 days at 60°C.

Infrared spectroscopy FTIR analysis
Fourier Transform Infrared Spectroscopy(FTIR) investigation was performed on modified hydroxyapatite with MWCNT-COOH. To examine the chemical composition of composite material, FTIR was performed to study the powder using a typical KBr pellet technique. The 15SrHA/CNT powders were grounded with KBr in the proportion of 1/150 (by weight) and pressed into a 3-mm pellet using a hand press. FTIR spectroscopy was performed on Nicolet Nexus

spectrophotometer with KBr discs in the $500–4000\,cm^{-1}$ region ($4\,cm^{-1}$ resolution, average 64 scans). FTIR investigation was performed on dry materials.

Morphological analysis
The morphological study to evaluate the dispersion of CNTs in the ceramic matrix was performed by transmission electron microscopy (TEM) and scanning electron microscopy (SEM) analyses. The TEM images were taken by a TEM FEI Tecnai G12 Spirit Twin model instrument operated at an accelerating voltage of 100 kV. Samples for TEM imaging were prepared by placing a drop of the aged Sr-HA with and without MWCNT-COOH suspensions (the suspensions were diluted in ethanol solution and dispersed by ultrasonic waves before use) onto carbon-coated copper grids, dried in air, and loaded into the electron microscope chamber.

The surfaces of 15SrHA/CNT gel materials were analyzed by SEM (JEOL 6310). For SEM analysis, the materials were mounted by a double adhesive tape to aluminum stubs. The stubs were sputter coated with gold to a thickness of around 20 nm. SEM analysis was performed at different magnification at 20 keV. X-ray energy dispersive spectroscopy (EDAX, Genesis 2000i) analysis was used for an approximate estimation of the Ca/P ratio.

Rheological properties
The rheological tests were carried out using HAAKE™ MARS™ Rheometer (Thermo Scientific) on gel materials with and without CNTs after an aging of 2 days at 60°C. At first, the linear viscoelastic region was determined with an amplitude sweep in the range 0.1–100 Pa at a constant frequency of 1.0 Hz. All the subsequent measurements were conducted within the linear viscoelastic regime, where the dynamic storage modulus (G') and loss modulus (G'') are independent of the strain amplitude. Frequency sweeps were performed from 0.1 to 10 Hz at 37°C and a constant strain of 10 Pa.

Bioactivity test
The bioactive properties of gel material (15SrHA/CNT) were investigated using a simulated body fluid (SBF) with ionic millimolar concentrations (Na^+ 142.0, K^+ 5.0, Ca^{2+} 2.5, Mg^{2+} 1.5, Cl^- 147.8, HCO_3^- 4.2, HPO_4^{2-} 1.0, SO_4^{2-} 0.5 mM) closely to those human plasma [7, 23]. The solution was prepared by dissolving each component NaCl, $NaHCO_3$, KCl, $MgCl_2$, HCl 1M, $CaCl_2 \cdot 6H_2O$ and Na_2SO_4 (ACS reagent grade, Sigma-Aldrich) in distilled water at 37°C and buffered at pH 7.4 using tris(hydroxymethyl)-aminoethane (Sigma-Aldrich, Italy). After 7days of incubation time, the 15SrHA/CNT gel material was washed with distilled water (3 times) and dried in the oven at 40°C overnight. The formation of hydroxyapatite deposits on the material surface was evaluated by SEM investigation.

Biological studies
In vitro elution materials and Alamar blue assay
The cytotoxicity analysis was performed by indirect test on the eluants. For this investigation, the materials (0.1 g) were incubated in medium Dulbecco's Mdified Eagle Medium (DMEM) (2.5 ml) for 3 and 5 days as reported in the ISO 10993-5 guidelines. After the incubation times, the eluants (100 μl) were placed in contact with 20 000 MG63 cell line and incubated for 48 h (exposure time). As control was considered the cells seeded on tissue culture plastic with DMEM solution without material eluant. The Alamar Blue assay was used to evaluate the cell viability through a redox phenomenon which gave a quantifiable indication of metabolic activity of live

cells [24]. After exposure time, medium was removed from the wells and a solution of Alamar Blue diluted 1:10 in phenol red-free medium was added to each well (500 µl) and incubated for a further 4 h at 37°C, 95% of humidity and 5% CO_2. The colorimetric analysis was performed on 100 µl of this solution in a 96-well plate ($n = 5$). Wells with a diluted Alamar blue solution and without any cells were used to correct for any background interference from the redox indicator. The absorbance was measured with a spectrophotometer (Victor X3, Perkin Elmer) at wavelengths of 570 and 600 nm. The cell viability is correlated with the magnitude of dye reduction and is expressed as percentage of AB reduction (%AB reduction), according to the manufacturer's protocol.

Cell proliferation

Cell proliferation assay was performed on human MSCs (hMSC) obtained from LONZA (Milano, Italy). hMSC were cultured in 75 cm^2 cell culture flask in Eagle's alpha minimum essential medium (α-MEM) supplemented with 10% fetal bovine serum, antibiotic solution (streptomycin 100 µg/ml and penicillin 100 U/ml, Sigma Chem. Co) and 2 mM L-glutamine and hMSCs from passages 5 were used for all the experimental procedures and incubated at 37°C in a humidified atmosphere (5% CO_2, 95% air). For cell proliferation, hMSC were plated at concentration of 1.6×10^4 cell/well in triplicate onto $0.5 \times 0.5 \times 0.5$ cm rounded of gel materials (with and without Sr) sterilized by autoclave at 121°C for 30 min. The cell proliferation was checked by using PicoGreen_dsDNA quantification kit (Invitrogen) for 7, 14 and 21 days of culture. The diluted dsDNA quantification reagent (100 µl) was added to 100 µl of cell lysates in a flat-bottomed, 96-well plate as reported in the protocol. After a mixing and incubation for 2–5 min at room temperature, protected from light, the fluorescence of Picogreen was determined at a wavelength of 520 nm after excitation at 585 nm using a spectrophotometer (Victor X3, Perkin-Elmer, Italy). The DNA concentration of samples was determined from the standard curve l-dsDNA standard.

Cell morphology

hMSC were seeded at 1×10^3 cell/ml onto $0.5 \times 0.5 \times 0.5$ cm rounded gel materials (0, 10, 15 and 20 mol%) Sr-HACNT and then incubated with the tested gel materials for 1 day. After this time, the non-attached cells were removed by careful washing with phosphate buffered saline (PBS) for three times and then incubated with cell tracker green CMFDA in phenol red-free medium at 37°C for 30 min. After that, cell culture was washed with PBS and incubated for 1 h in complete medium. The interaction of hMSC onto gel materials in terms of morphology and cell spreading was evaluated by confocal laser scanning microscopy (LSM 510, CarlZeiss).

Total intracellular protein content

To evaluate the intracellular protein content, hMSC 1.6×10^4 cell/well were seeded onto the gel materials and were cultured in α-MEM supplemented with 10% fetal bovine serum, antibiotic solution (streptomycin 100 µg/ml and penicillin 100U/ml, Sigma Chem. Co) and 2 mM L-glutamine for 7, 14 and 21 days. At the end of the incubation time, hMSCs were lysed using 1X lysis buffer with 0.2% of Triton X-100. Total protein content in the cell lysates was determined spectrophotometrically using a commercially available kit (Pierce Chemical Co.) and following manufacturer's instructions. Briefly, aliquots of each sample were incubated with a solution of copper sulfate and bicinchoninic acid at 37°C for 30 min. The absorbance at 562 nm was measured by a spectrometer Victor X3 (Perkin Elmer, Italy). Total

intracellular protein (expressed as µg) synthesized by hMSC cultured on the gel materials at different composition was determined from a standard curve of absorbance versus specific concentrations of bovine serum albumin BSA measured in parallel with experimental samples. All experiments were repeated twice, and three gel materials were used in each experiment.

Colorimetric ALP activity assay

The differentiation of hMSC was tested by measuring their Alkaline Phosphatase (ALP) activity upon culture onto gel materials after 7, 14 and 21 days (SensoLyte pNPP ALP assay kit, ANASPEC, Milano, Italy). At the end of each time point, cultures were washed gently with PBS followed by washing twice with cold 1X assay buffer (BD Biosciences, Milano, Italy). To evaluate the ALP activity onto the cell lysates (50 µl), the cultures were treated with 1X lysis buffer with 0.2% of Triton X-100. The absorbance of samples was measured in a 96-well plate at 405 nm and ALP values were normalized by milligrams of total protein content determined as described above. ALP experiments were repeated twice and three gel materials were used in each experiment.

RT-polymerase chain reaction

Total RNA was extracted from CaP gels reinforced with CNT using a Trizol reagent (Sigma) after 21 days of culture for gene expression of bone-related markers. The contaminating DNA was removed by treating with DNase I (Life Technologies, Italy) before that Reverse Transcription Polymerase chain reaction (RT-PCR) was performed. The absorbency at 260/280 nm was measured to determine the RNA concentration. One microgram of total RNA was used to perform one-step RT-PCR reaction (Life Technologies, Italy) according to the manufacturer's protocol. Briefly, cDNA synthesis program was 1 cycle at 60°C for 30 min followed of denaturation cycle of 94°C for 2 min. cDNA was amplified at 94°C for 15 s, 55°C for 30 s and 68°C for 1 min for 35 cycles in a thermal cycler (Applied Biosystem). Primers used for amplification of bone-related molecules were upstream and downstream as follows: osteopontin (OPN) 5′-TTCGGATGAG TCTGATGAGACC-3′, 5′-GGAAGAACAGAAGCAAAGTGC-3′, osteocalcin (OCN) 5′-CAGCAGAGCGACACCCTAGACC-3′, 5′-CATGAGAGCCCCTCACACTCC-3′, ALP 5′-GGAGGGACCC TCGCCAGTGCT-3′ 5′-AGAGGGCCACGAAGGGGAACT-3′ and glyceraldheyde-3-phosphate dehydrogenase (GAPDH) 5′-CCACCCA TGGCAAATTCCATGGCA-3′, 5′-TCTAGACTGGCAGGTCAG GTCCACC-3′ was utilized as housekeeping gene. Reaction products were separated using gel electrophoresis on 1.2% agarose gel stained with ethidium-bromide. The semi-quantitative analyses were subject to image density of amplified bone-related PCR products in the Gel-Quant express of DNR Bio-imaging System. The data obtained were represented as a relative ratio of the respective PCR product against the GAPDH PCR product.

Results

Synthesis of gels materials

Injectable strontium-modified CaP gels reinforced with modified CNTs (SrHA/MWCNT-COOH) were successfully synthesized by sol–gel method (Fig.1). A preliminary investigation showed a difference in the gelification time of the biomaterials prepared at different Sr concentration as reported in our previous study [7]. Briefly, gels prepared at 0 and 10 mol% of Sr reached a final setting after 1 h of stirring at 40°C. Meanwhile, the gels prepared at 15 and 20 mol%

of Sr showed a slight delay, their gelation time was achieved after 2–3 h. This different behavior probably is due by the ionic substitutions in the crystallographic positions of the hydroxyapatite lattice that generally cause changes in the values of the cell parameters dependent on the different sizes and amount of the ions [7]. However, all gels synthesized at room temperature could be successfully equilibrated at pH 7.4 without any significant dissolution thus ensuring their compatibility with biological systems (Figs 5-8).

Infrared spectroscopy FTIR analysis

Figure 2 shows the FTIR spectrum of 15SrHA/CNT sample dried in the oven for 2 days at 40°C. The bands at 564 and 605 cm^{-1} were attributed to P-O bending of phosphate group and at 1117 cm^{-1} was assigned to PO_4 corresponding to different vibration modes of phosphate group in HA. Meanwhile, the bands at 889 and 736 cm^{-1} were referred to HPO_4^{2-} and $P_2O_7^{2-}$ as reported in our previous study [7]. The bands at 3424 and 3190 cm^{-1} were attributed to stretching vibrations of OH group. The oxidation forming the COOH groups on the MWCNTs surface determines the development of three distinct peaks (C=O, O–H, C–O). In fact, an absorption band at 1762 cm^{-1} is corresponding to C=O stretching of COOH, while the absorption bands at 1386 cm^{-1} and 1078 cm^{-1} are associated with O–H bending and C–O stretching, respectively [25]. Moreover, in the FTIR spectra appears a band at 1397 cm^{-1} [26] due to ν_3 stretching mode of CO_3^{2-} groups. However, carbonates are constituents of bone structures [27] and the presence of CO_3^{2-} in the gel materials could increase the bioactive properties of HA.

The absorption bands at 1637 cm^{-1} and 824 cm^{-1} are more likely from the C=C stretching mode of CNTs. As a result, chemical interaction between the chemical group of MWCNTs and cations of the HA particles can be produced, such as –COO-Ca-OOC.

Morphological investigation and bioactivity test

Figure 3(I) shows TEM images of MWCNT and biomineralized MWCNT (HA/CNT and 15SrHA/CNT). It is evident that the surface of MWCNT is smooth and clean; meanwhile, on the biomineralized MWCNT surface, needle-like nanoparticles were formed. In particular, TEM image of 15SrHA/CNT system shows a presence of CNTs network decorated with modified-hydroxyapatite nanoparticles; any copious clusters appear in the system.

Furthermore, SEM imaging performed on 15SrHA/CNT (0.5 wt%) (Fig. 3A-II) composite material demonstrated a homogeneous dispersion of nanotubes in ceramic matrix with any presence of agglomerates.

The EDAX analysis shows (Fig. 3B-II) that the CaP precipitated during the sol–gel synthesis is composed mainly of hydroxyapatite, with a Ca/P molar ratio of about 1.65. This result is important for the bioactive properties of material. In fact, some SEM observations performed on SrHA/CNT, incubated for a shorter time (7 days) in a SBF solution further revealed that the composite material shows a good bioactivity with the presence of numerous apatite depositions on the 15SrHA/CNT gel materials may be directly correlated to the presence of HA nanoparticles which appear as bioactive nucleation sites (Fig. 3C-II). Moreover, the presence of CNTs do not reduce the bioactive potential of composite materials as demonstrating by a presence of rose petal-like apatite crystallites (Fig. 3D-II) on the material surface.

Rheological properties

Frequency sweep tests were carried out in the linear viscoelastic region. The results demonstrated that G′ values are higher than G″ values at 37°C because the tested materials were analyzed after gelification and aging of 2 days at 60°C. Furthermore, an increasing of one order of magnitude for G′ modulus after addition of multiwall CNTs was observed (Fig. 4A). MWCNT changes the tridimensional network of gel and a new arrangement between the HA nanoparticles and CNTs was obtained, as also observed in the TEM images. Meanwhile when the Sr^{2+} was used to replace Ca^{2+}, G′ value is lower than the G′ value of HA gel (Fig. 4B). This behavior probably is due to an increasing of cell volume of doped nanoparticles (10, 15 and 20 mol%) [7]. In fact, increasing strontium substitution for calcium in the HA structure determines a linear variation in the cell parameters in agreement with the mean dimension of the cation.

After nanotubes addition to SrHA systems, an improvement of elastic modulus of 20SrHA gel than (10–15)SrHA/CNT systems was obtained. The storage modulus (G′) can be considered as a measure of the extension of the gel network formation and higher values for G′ means a stronger gel [28].

Biological studies

In this study, the cytotoxicity evaluation of 15SrHA/CNT gel material using MG63 cell line was performed on eluants (3 and 5 days) after 48 h of exposure time (Fig. 5). The biocompatibility of the material was determined quantitatively using a method which assessed cell metabolic function and proliferation (Alamar blue). The results demonstrated that the material does not release any toxic component with a negative effect on metabolic activity of MG63. Furthermore, it was observed an increasing cell response with increased the strontium amount released from gel material. Figure 6 shows the effect of the materials on hMSC cell adhesion after 1 day of cell culture. The cellular attachment is the first step in evaluating the biocompatibility of hMSC onto the SrHA/CNT composite materials. It was demonstrated that hMSC cells show a good compatibility and affinity for the SrHA/CNT gel materials demonstrating a smooth and elongate morphology over the material surface. Our results also demonstrated that a good cell attachment and spreading was observed for HA/CNT indicating that the presence of CNTs does not negate cellular behavior. Figure 7 shows the amount of DNA (ng) produced by hMSC after 7, 14 and 21 days of culture. As reported in the results, the cell proliferation of systems was typical of the negative control samples. Total DNA has shown that HA/CNT series has a positive influence on cellular growth when compared to the control samples thus complementing the results in Figs 5 and 7. In addition, the composite materials 10 and 15SrHA/CNT show the best proliferation results in the first 7 and 14 days and the best production of intracellular protein content until the day 21 (Fig.8). These results demonstrate that the combination of Sr^{2+} ions and HA/CNT in the bioceramic system has a real positive influence on hMSC proliferation rate.

The ALP activity was determined on cell cultures and as early as 7 days (Fig. 9). A time point which can exhibit the production of the early marker of osteogenic differentiation. ALP activity showed that at 7 and 14 days, a high enzymatic activity on HA/CNT doped with 10 and 15%mol. In this data, the composite with highest value of Sr and MWCNT-COOH (20SrHA/CNT) showed the lowest value of ALP probably due to an early onset of the mineralization process. However, at 21 days of culture, there is a tendency for less activity in ALP activity due to the late phases of osteogenesis, though activity was still observed on the 10SrHA/CNT material.
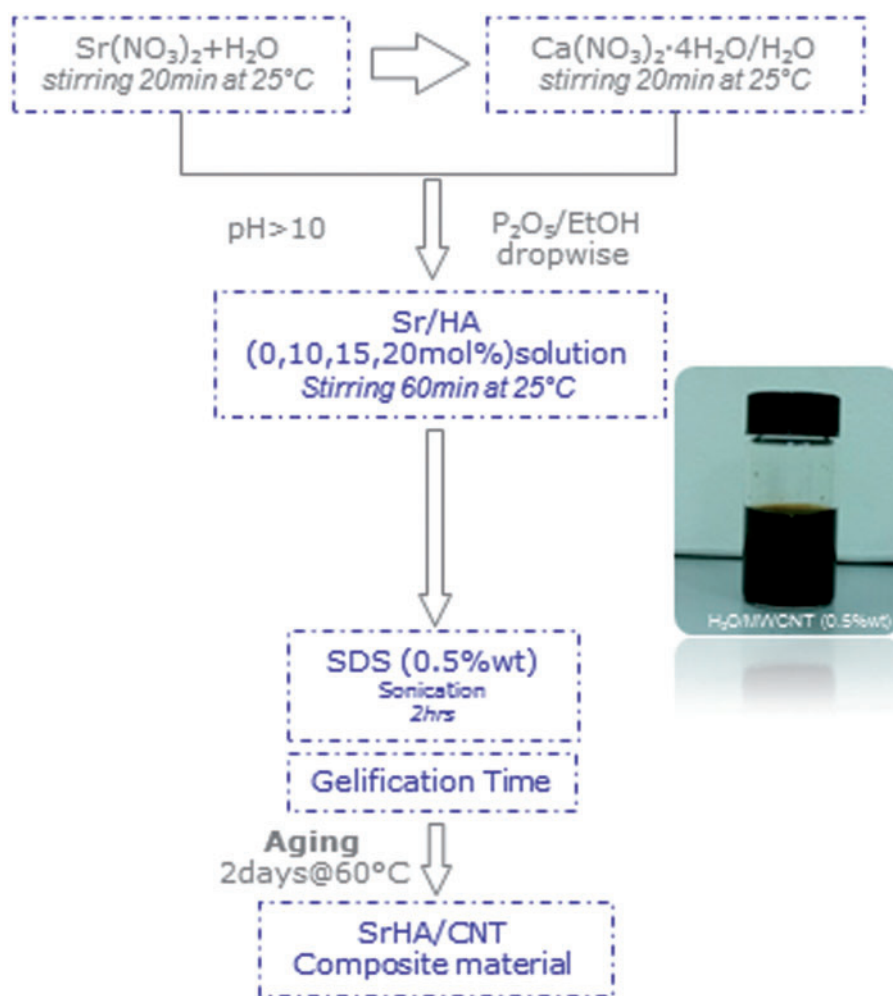
Figure 1. Flowchart of SrHA/CNT composite material synthesized by sol–gel method

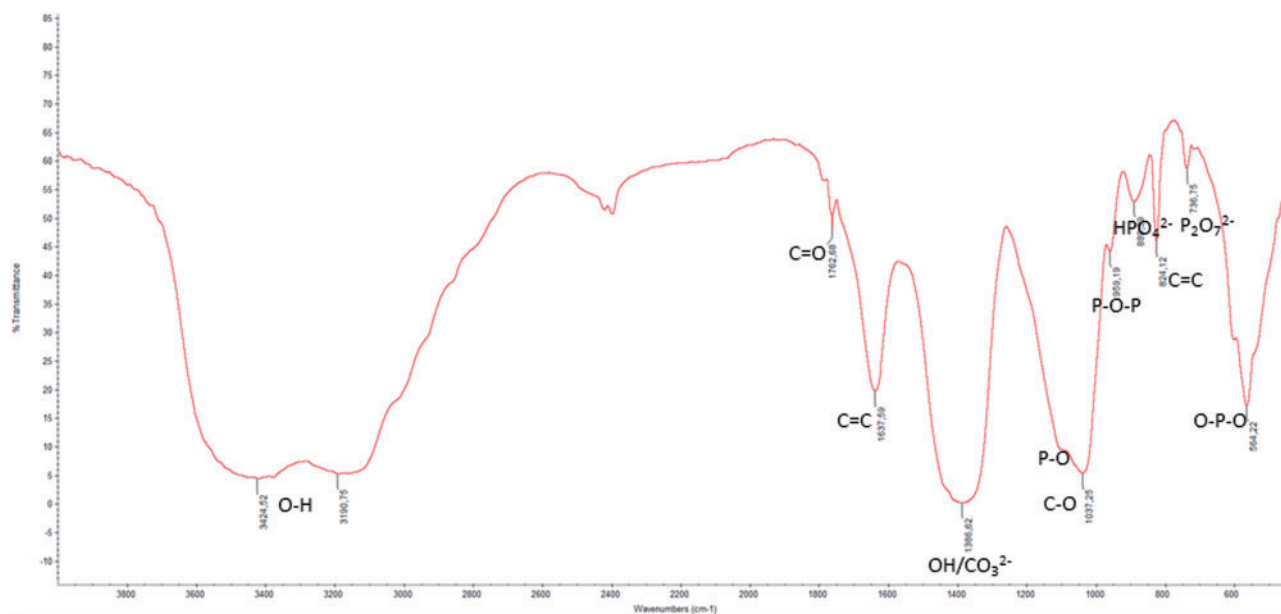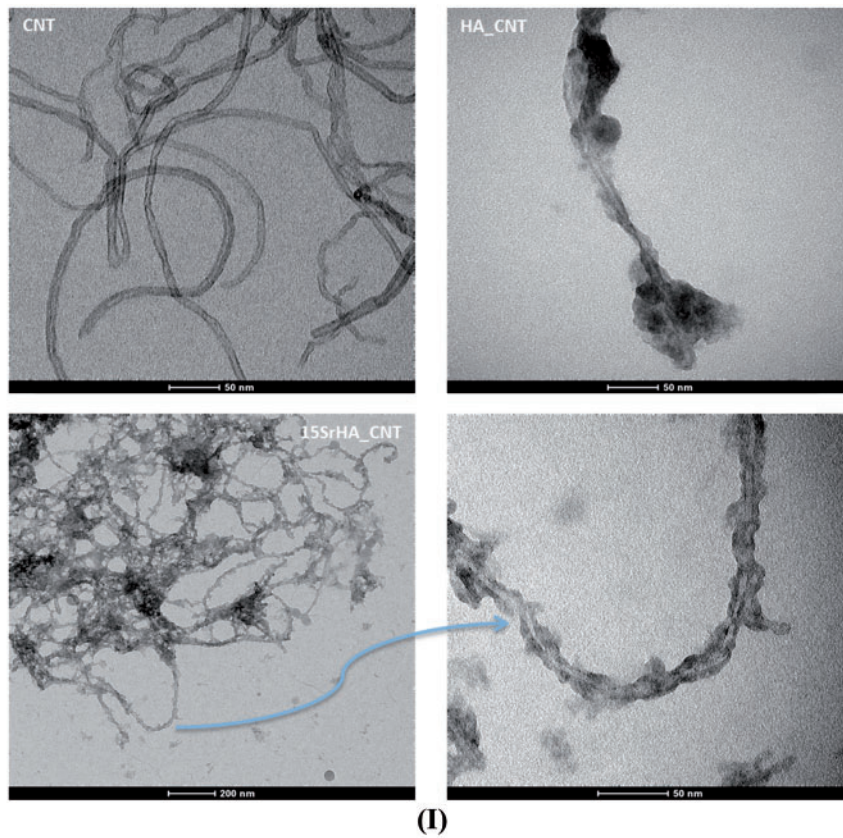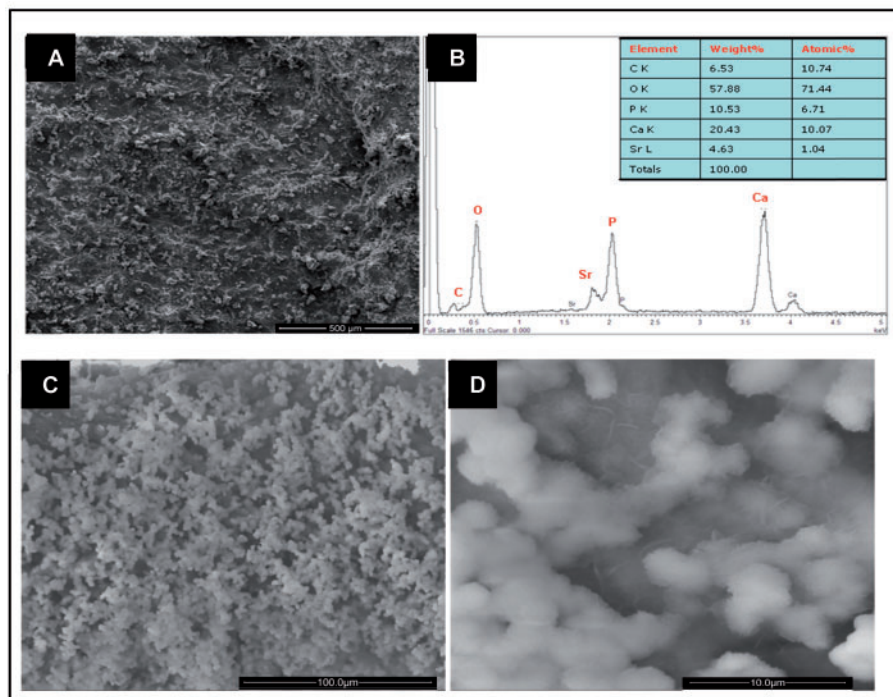**Figure 2.** FTIR of 15SrHA/CNT gel material synthesized at room temperature

(I)

Element	Weight%	Atomic%
C K	6.53	10.74
O K	57.88	71.44
P K	10.53	6.71
Ca K	20.43	10.07
Sr L	4.63	1.04
Totals	100.00	

(II)

Figure 3. (**I**) TEM images of CNT, HA/CNT and 15SrHA/CNT at different magnification dissolved in ethanol solution. (**II**) SEM images of 15SrHA/CNT (**A**) and EDS analysis performed on Strontium-doped hydroxyapatite (**B**). SEM images at different magnification (**C** and **D**) of 15SrHA/CNT after SBF treatment
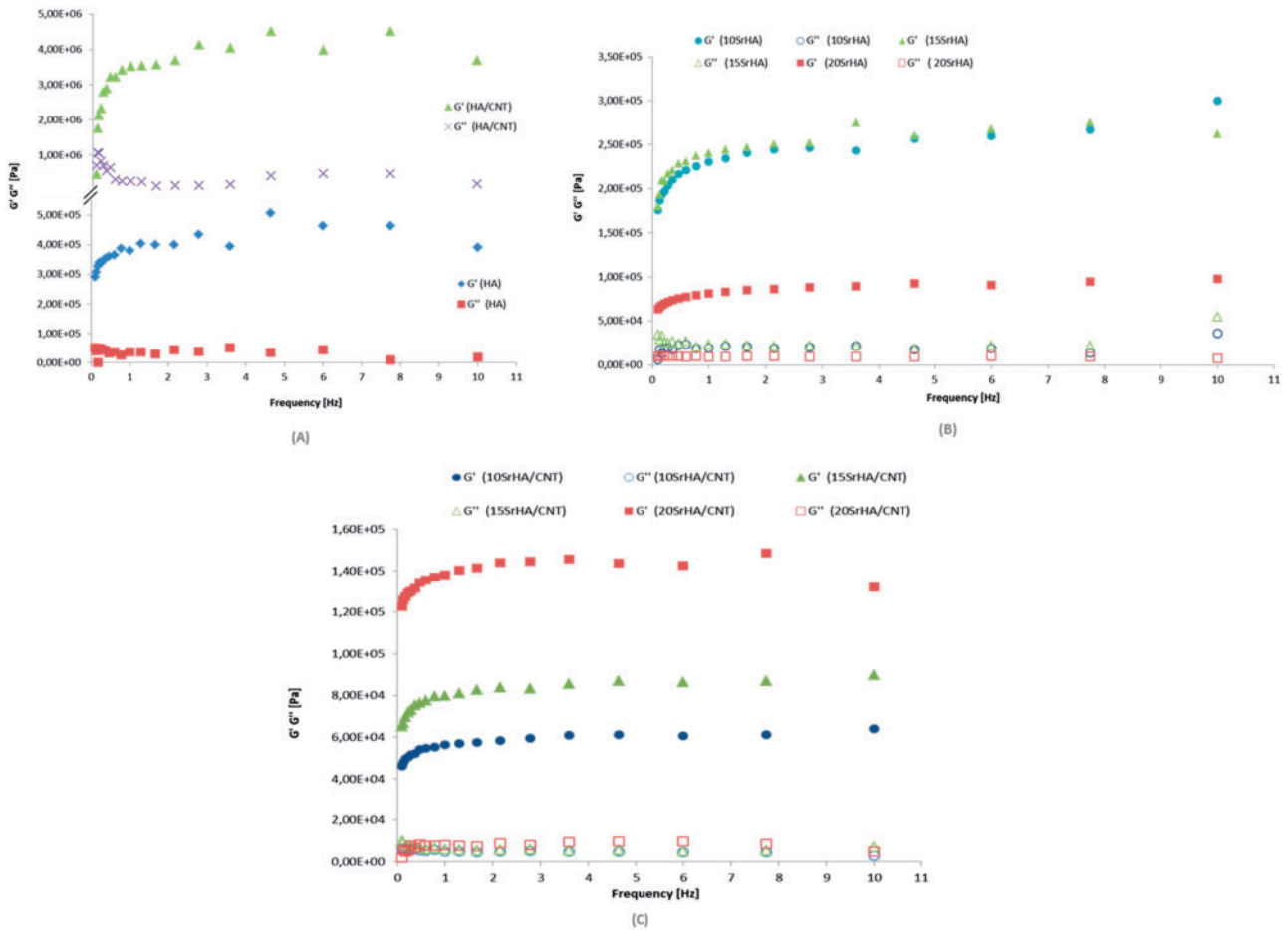
Figure 4. Frequency sweep for HA and HA/CNT (**A**), 10–15 and 20 SrHA gels (**B**), 10–15 and 20 SrHA/CNT 0.5 wt% gels at 37°C (**C**). Frequency sweeps were performed from 0.1 to 10 Hz at 37°C and a constant strain of 10 Pa
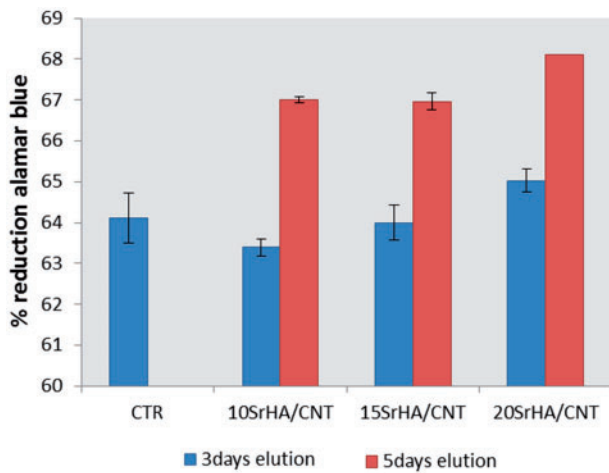
Figure 5. *In vitro* elution study by indirect contact after 48 h of exposure time

The expression of several bone-related transcripts was also examined after 21 days of culture. Figure 10 shows that HA/CNT doped with strontium significantly improves the osteogenic differentiation by the expression of early (ALP and osteopontin OPN) and late (osteocalcin OCN) markers. Our results indicate that 10SrHA/CNT showed high up-regulation of ALP, OPN when comparing

with 15SrHA/CNT and 20SrHA/CNT. Moreover, the up-regulation of these early markers on all CaP gels are highly expressed (Fig. 10A and B). However, in the three CaPs: 10SrHA/CNT, 15SrHA/CNT and 20SrHA/CNT, the osteocalcin expression was faintly detected as we can observe on the histogram where the semi-quantified expression showed a very low relative expression comparing against the control GAPDH PCR product.

Discussion

Composite materials based on strontium-modified hydroxyapatite reinforced with carboxylate multiwall CNTs were created by *in situ* synthesis using sol–gel technology. This approach was based on a simple mechanism where the carboxyl groups present on the nanotubes may play an essential part in anchoring calcium ions. To obtain a good nucleation of HA nanoparticles in MWCNT-COOH, *in situ* preparation was performed at high pH value (pH > 10) followed by an aging step of 2 days at 60°C. The alkali treatment promotes the deprotonation of carboxyl groups ($-COOH$) on the MWCNT ionizing them and improving the interaction between the MWCNT substrates and HA nanoparticles. The process was combined with a sonication treatment (2 h) using sodium dodecyl sulfate as a dispersant agent enhancing the distribution of nanotubes in the HA matrix. Furthermore, during the synthesis process when MWCNT-COOH solution was introduced into the Ca/Sr solution,
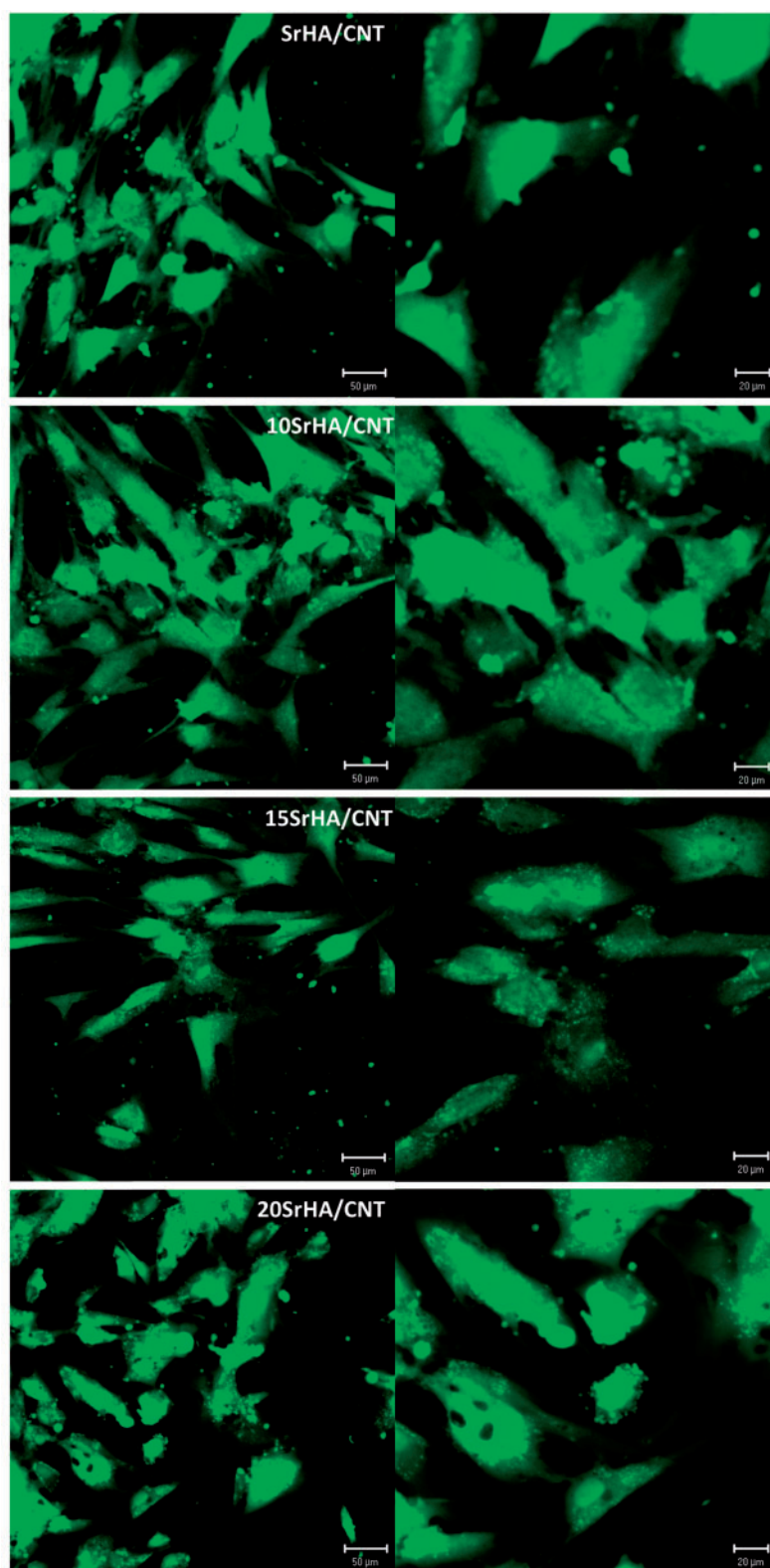
Fig.6

Figure 6. Confocal images of hMSCs adhesion on (10–15 and 20 mol%) SrHA/CNT gel materials after culturing for 24hrs

the Ca^{2+} cations could interact with oxygen atoms by electrostatic interactions and functioned as the sites for the nucleation and crystallization of the HA particles. In fact, the Ca^{2+} could react *in situ* with the ambient drop wise phosphate ions via electrovalent bonds to form HA nanoparticles as reported in other studies [29, 30]. After mixing and aging steps, SrHA/CNT systems showed a different behavior than the materials without CNT. To increasing the Sr amount, an addition of CNTs in the systems determines an
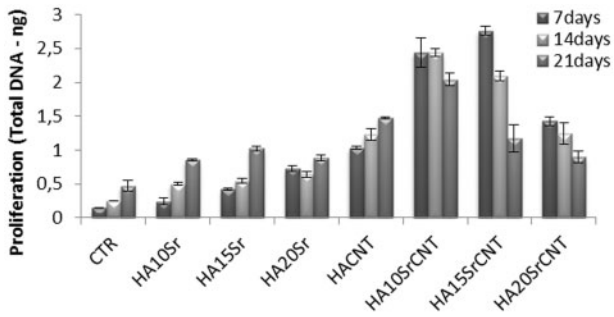
Figure 7. DNA picogreen assay of hMSC after 7, 14 and 21 days of cell culture. Results were considered to be significant at $P < 0.05$
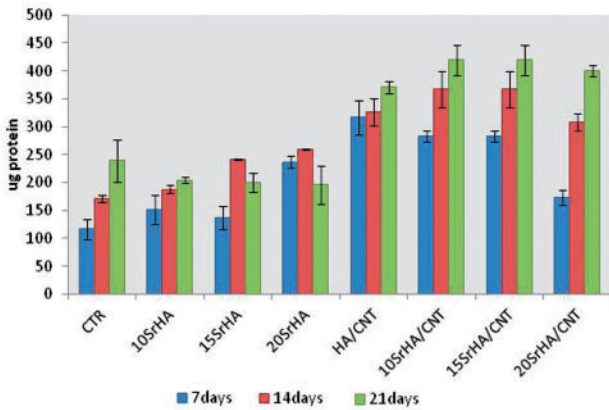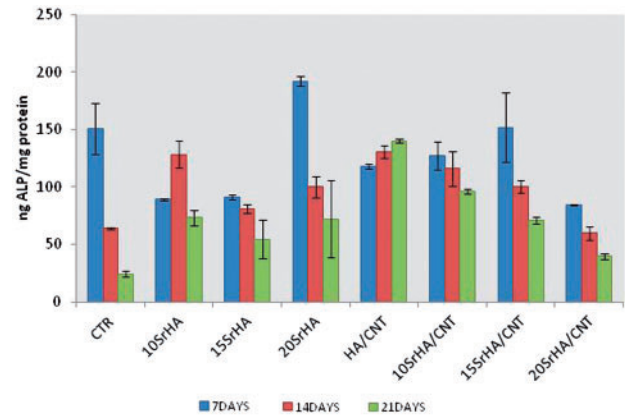

Figure 8. Total intracellular protein content by microBCA of hMSCs on gel materials at 7, 14 and 21 days of cell culture

Figure 9. ALP activity normalized on milligrams of proteins at 7, 14 and 21 days of incubation time in basal medium. Results were considered to be significant at $P < 0.05$

improvement of elastic modulus G′ SrHA/CNT gels become strongly viscoelastic solid-like materials $(G' > G'')$ which can be suitably shaped and injected to fill micropores in a bone defect. This behavior could be obtained by the chemical interactions and the distribution of SrHA nanoparticles along the CNTs.

The interaction between COO^- and Ca^{2+} groups were evaluated by FTIR analysis (Fig. 2), and the presence of surfactant allows a homogeneous material to be obtained as demonstrated in morphological analyses (Fig. 3). Moreover, the EDAX analysis (in the square of Fig. 3B) showed that the atomic ratio Ca + Sr/P is 1.65, close to that of natural bone, which have been reported to provide the biocomposites with higher bioactivity [31].

The toxicity of CNT in medical materials is under scrutiny. The results from Pulskamp et al. [32] demonstrated that CNTs have no acute toxicity effect but induced intracellular reactive oxygen species (oxygen radicals) and it is dependent on contaminants. Meanwhile, Wick et al. [33] reported that the degree and kind of agglomeration (i.e. rope-like agglomerates) influenced the cytotoxicity of CNTs, as showed by the effects on cell growth. It was also found that the presence of CNTs has good effect on attachment and spreading of osteoblast cells [34] and also on the improvement of bioactive properties of the CNTs-containing composites [35–38].

Here, we have evaluated that the eluants obtained from SrHA/CNT containing 10, 15 and 20 mol. (%) and 0.5%wt of MWCNT-COOH after 3 and 5 days of elution time had good biocompatibility on MG63 cells. Those results demonstrated that the paste-like materials do not release any toxic components and the amount of CNTs and surfactant used during the synthesis are compatible with the

observed cell metabolic activity. Furthermore, our results have shown that the presence of MWCNT stimulates not only cell proliferation but also induces the intracellular protein production. Nayak et al. [39] demonstrated that surface roughness of CNT thin films may effect on proteins adsorption on the material surface with a successive effect on cellular behavior in terms of proliferation and differentiation of hMSCs into bone lineage. Moreover, a recent study [40] reported that MWCNT has beneficial effects on bones when they are used as biomaterials inhibiting osteoclastic bone resorption in vivo and suppressed a transcription factor essential for osteoclastogenesis in vitro.

The phosphatase activity (ALP) is one of the most widely used markers for osteogenic differentiation, and the enzymatic activity is considered a necessary prerequisite for the onset on mineralization [41–43]. Here, we demonstrated that the gel materials cultured with MSCs in vitro increased the cell proliferation, cell protein production and significantly induced osteogenic differentiation, thus promoting the ALP activity and the expression of some bone-related molecules as OPN and OCN. Concerning the ALP, a membrane-bound ectoenzymes that hydrolyze monophosphate esters at a high pH, our preliminary studies analyzing the differentiation of MSCs toward the osteoblastic-like phenotype was determined using the p-nitrophenyl phosphate method. The results showed a constant increase in ALP activity confirming the ability of the injectable strontium-modified CaP gels reinforced with CNTs to support MSC differentiation toward the osteoblast-like phenotype and in future could support the ECM mineralization. Moreover, our analysis of gene expression showed that MSCs underwent differentiation when cultured onto the injectable strontium-modified CaP gels reinforced with CNT material and we could detect the transcripts for ALP, OPN and slightly of OCN transcript. Osteopontin is a multifunctional extracellular phosphorylated glycoprotein recognized as a key molecule that could play an important role in multiple biological processes and is essential for the mineralization process of bone because this protein is involved as regulator of the crystal growth in the mineralization front and bone turnover [44, 45]. Osteocalcin plays a role in the bone mineralization and in the calcium ion homeostasis. This protein secreted only by osteoblasts has a strong binding affinity to calcium ions and HA due to the presence of glutamic acid rich regions in its chemical structure [46, 47]. Our experimental results revealed that gene expression was temporally and spatially regulated most likely by the physico-chemical aspect of
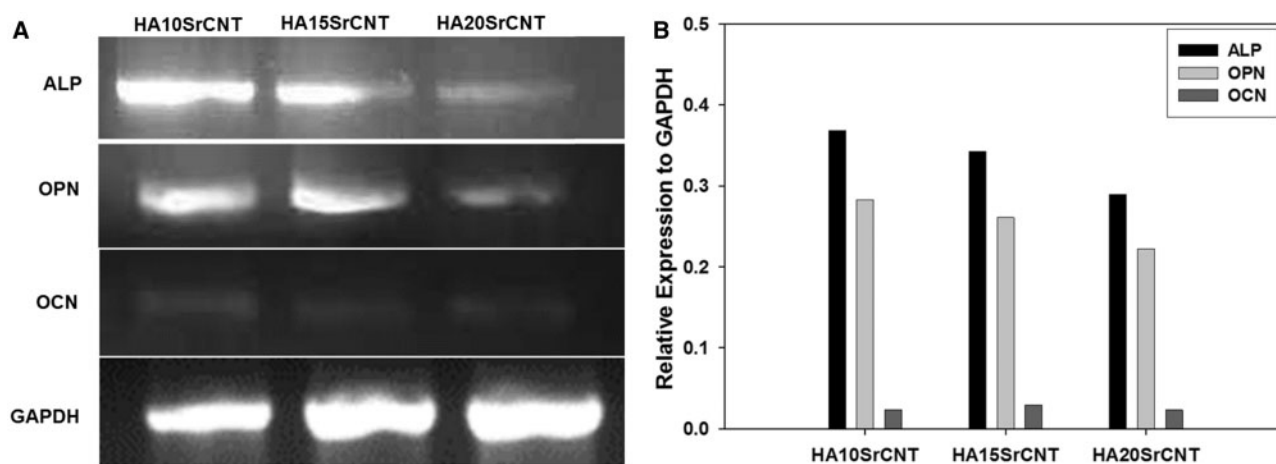
Figure 10. Gene expression of SrHA/CNT gel materials after 21 days of culture in α-MEM (**A**). Semi-quantitative analysis represented as a ratio of the respective PCR product/GAPDH PCR product (**B**)

composite material and this could be supported by some reports that suggest an important role of the physical properties of the material and also that cells treated with only synthetic apatite or CaP materials are induced and responding to express significant amounts of OPN [48, 49]; however, OCN has been classified as the last of expression markers in mature osteoblasts and in our study is observed that there is faint signal suggesting that MSC responded to the composite material and had at least entered into a maturation stage [50,51]. However, further studies are needed to investigate the effective mechanism of action of gel composite material on the bone remodeling to reducing the osteoclast growth.

Conclusions

In this study, injectable materials based on multiwall CNTs reinforced strontium-substituted hydroxyapatite at different compositions have been synthesized by sol–gel approach. The products showed a homogenous dispersion of nanotubes in the ceramic matrix that is important to control the rheological and bioactive properties. Furthermore, the presence of carboxyl nanotubes combined with strontium improved the cellular behavior in terms of adhesion and proliferation. In fact, gel materials with MWCNT-COOH and higher amount of Strontium (HA-10Sr, HA-15Sr and HA-20Sr) induced osteogenic differentiation, thus promoting the ALP activity and the expression of some bone-related molecules as OPN and OCN. Further studies are required to evaluate *in vivo* the potential benefits of Sr-HA/CNT as a bone substitute biomaterial and its potentially effect for osteoporosis treatment.

Acknowledgements

Funding

References

1. Renaudin G, Laquerrière P, Filinchuk Y *et al*. Structural characterization of sol–gel derived Sr-substituted calcium phosphates with anti-osteoporotic and anti-inflammatory properties. *J Mater Chem* 2008; **18**:3593–600.

2. Zhang W, Shen Y, Pan H *et al*. Effects of strontium in modified biomaterials. *Acta Biomater* 2011; **7**:800–8.

3. Peng S, Zhou G, Luk KDK *et al*. Strontium promotes osteogenic differentiation of mesenchymal stem cells through the Ras/MAPK signalling pathway. *Cell Phys Biochem* 2009; **23**:165–74.

4. Jegou Saint-Jean S, Camirè CL, Nevsten P *et al*. Study of the reactivity and in vitro bioactivity of Sr-substituted α-TCP cements. *J Mater Sci Mater Med* 2005; **16**:993–1001.

5. Tan S, Zhang B, Zhu X *et al*. Deregulation of bone forming cells in bone diseases and anabolic effects of strontium-containing agents and biomaterials. *Biomed Res Int* 2014; **2014**:12.

6. Schumacher M, Lode A, Helth A *et al*. A novel strontium(II)-modified calcium phosphate bone cement stimulates human-bone-marrow-derived mesenchymal stem cell proliferation and osteogenic differentiation in vitro. *Acta Biomater* 2013; **9**:9547–57.

7. Raucci MG, Giugliano D, Alvarez-Perez MA *et al*. Effects on growth and osteogenic differentiation of mesenchymal stem cells by the strontium-added sol–gel hydroxyapatite gel materials. *J Mater Sci: Mater Med* 2015; **26**:90–101.

8. Bohner M, Baroud G. Injectability of calcium phosphate pastes. *Biomaterials* 2005; **26**:1553–63.

9. Dos Santos LA, De Oliveira LC, Rigo ECD *et al*. Fiber reinforced calcium phosphate cement. *Artif Organs* 2000; **24**:212–6.

10. Wang XP, Ye JD, Wang YJ *et al*. Reinforcement of calcium phosphate cement by bio-mineralized carbon nanotube. *J Am Ceram Soc* 2007; **90**:962–4.

11. Iijima S. Helical microtubules of graphitic carbon. *Nature* 1991; **354**:56–8.

12. Treacy MMJ, Ebbesen TW, Gibson JM. Exceptionally high Young's modulus observed for individual carbon nanotubes. *Nature* 1996; **381**:678–80.

13. Gojny FH, Nastalczyk J, Roslaniec Z *et al*. Surface modified multi-walled carbon nanotubes in CNT/epoxycomposites. *Chem Phys Lett* 2003; **370**:820–4.

14. Gheith MK, Sinani VA, Wicksted JP *et al*. Single-walled carbon nanotube polyelectrolyte multilayers and freestanding films as a biocompatible platform for neuroprosthetic implants. *Adv Mater* 2005; **17**:2663–70.

15. Boccaccini AR, Gerhardt LC. Carbon nanotube composite scaffolds and coatings for tissue engineering applications. *Key Eng Mater Adv Bioceram Med Appl* 2010; **441**:31–52.

16. Shi XF, Hudson JL, Spicer PS *et al*. Injectable nanocomposites of single-walled carbon nanotubes and biodegradable polymers for bone tissue engineering. *Biomacromolecules* 2006; 7:2237–42.

17. Peigney A. Composite materials: tougher ceramics with nanotubes. *Nature Mater* 2003; 2:15–16.

18. Ma RZ, Wu J, Wei BQ *et al*. Processing and properties of carbon nanotubes-nano-SiC ceramic. *J Mater Sci* 1998; 33:5243–6.

19. Zhang W, Liao SS, Cui FZ. Hierarchical self-assembly of nano-fibrils in mineralized collagen. *Chem Mater* 2003; 15:3221–6.

20. Lee HH, Shin US, Jin GZ *et al*. Highly homogeneous carbon nanotube-polycaprolactone composites with various and controllable concentrations of ionically modified-MWCNTs. *Bull Korean Chem* 2011; 32:157–61.

21. Balàzsi C, Kònya Z, Wèber F *et al*. Preparation and characterization of carbon nanotube reinforced silicon nitride composites. *Mater Sci Eng C* 2003; 23:1133–7.

22. Xia Z, Riester L, Curtin WA *et al*. Direct observation of toughening mechanisms in carbon nanotube ceramic matrix composites. *Acta Mater* 2004; 52:931–44.

23. Kokubo T, Hiroaki T. How useful is SBF in predicting in vivo bone bioactivity? *Biomaterials* 2006; 27:2907–15.

24. Sephra NR. Multiple applications of Alamar Blue as an indicator of metabolic function and cellular health in cell viability bioassays. *Sensors* 2012; 12:12347–60.

25. Her SC, Lai CY. Dynamic behavior of nanocomposites reinforced with multi-walled carbon nanotubes (MWCNTs). *Materials* 2013; 6:2274–84.

26. Slósarczy A, Paszkiewic Z, Paluszkiewicz C. FTIR and XRD evaluation of carbonated hydroxyapatite powders synthesized by wet methods. *J Mol Struct* 2005; 744:657–61.

27. Murugan R, Ramakrishna S. Development of nano composites for bone grafting. *Compos Sci Technol* 2005; 65:2385–406.

28. Deng G, Tang C, Li F *et al*. Covalent cross-linked polymer gels with reversible sol−gel transition and self-healing properties. *Macromolecules* 2010; 43:1191–4.

29. Cazorla C, Rovira C, Rojas V. Calcium-based functionalization of carbon nanostructures for peptide immobilization in aqueous media. *J Mater Chem* 2012; 22:19684–93.

30. Zhao L, Gao L. Novel in situ synthesis of MWNTs-hydroxyapatite composites. *Carbon* 2004; 42:423–6.

31. Raucci MG, Guarino V, Ambrosio L. Hybrid composite scaffolds prepared by sol–gel method for bone regeneration. *Compos Sci Technol* 2010; 70:1861–8.

32. Pulskamp K, Diabate S, Krug HF. Carbon nanotubes show no sign of acute toxicity but induce intracellular reactive oxygen species in dependence on contaminants. *Toxicol Lett* 2007; 168:58–64.

33. Wick P, Manser P, Limbach LK *et al*. The degree and kind of agglomeration affect carbon nanotube cytotoxicity. *Toxicol Lett* 2007; 168:121–31.

34. Aoki N, Yokoyama A, Nodasaka Y *et al*. Cell culture on a carbon nanotube scaffold. *Biomed Nanotech* 2005; 1:402–5.

35. White AA, Best SM, Kinloch IA. Hydroxyapatite–carbon nanotube composites for biomedical applications: a review. *Int J Appl Ceram Technol* 2007; 4:1–13.

36. Balani K, Anderson R, Laha T *et al*. Plasma-sprayed carbon nanotube reinforced hydroxyapatite coatings and their interaction with human osteoblasts in vitro. *Biomaterials* 2007; 28:618–24.

37. Chen Y, Zhang YQ, Zhang TH *et al*. Carbon nanotube reinforced hydroxyapatite composite coatings produced through laser surface alloying. *Carbon* 2006; 44:37–45.

38. Li A, Sun K, Dong W *et al*. Mechanical properties, microstructure and histocompatibility of MWCNTs/HAp biocomposites. *Mater Lett* 2006; 61:1839–44.

39. Nayak TR, Jian L, Phua LC *et al*. Thin films of functionalized multiwalled carbon nanotubes as suitable scaffold materials for stem cells proliferation and bone formation. *ACS Nano* 2010; 4:7717–24.

40. Narita N, Kobayashi Y, Nakamura H *et al*. Multiwalled carbon nanotubes specifically inhibit osteoclast differentiation and function. *Nano Lett* 2009; 9:1406–13.

41. Ren Z, Do LD, Bechkoff G *et al*. Direct determination of phosphatase activity from physiological substrates in cells. *PLoS One* 2015; 10:e0120087. doi:10.1371/journal.pone.0120087.

42. Millan JL. The role of phosphatases in the initiation of skeletal mineralization. *Calcif Tissue Int* 2013; 93:299–306.

43. Orimo H. The mechanism of mineralization and the role of alkaline phosphatase in health and disease. *J Nippon Med Sch* 2010; 77:4–12.

44. Bouleftour W, Bouet G, Granito RN *et al*. Blocking the expression of both bone sialoprotein (BSP) and osteopontin (OPN) impairs the anabolic action of PTH in mouse calvaria bone. *J Cell Phys* 2015; 230:568–77.

45. Rajachar RM, Truong AQ, Giachelli CM. The influence of surface mineral and osteopontin on the formation and function of murine bone marrow derived osteoclasts. *J Mater Sci Mater Med* 2008; 19:3279–85.

46. Wei J, Karsenty G. An overview of the metabolic functions of osteocalcin. *Curr Osteoporos Rep* 2015; 13:180–5.

47. Oldknow KJ, MacRae VE, Farquharson C. Endocrine role of bone: recent and emerging perspectives beyond osteocalcin. *J Endocrinol* 2015; 225:R1–19.

48. Ling LE, Lin F, Hong-Chen L *et al*. The effect of calcium phosphate composite scaffolds on the osteogenic differentiation of rabbit dental pulp stem cells. *J Biomed Mater Res A* 2015; 103A:1732–45.

49. Duan W, Ning C, Tang T. Cytocompatibility and osteogenic activity of a novel calcium phosphate silicate bioceramic: silicocarnotite. *J Biomed Mater Res A* 2013; 101A:1955–61.

50. Zhu JX, Sasano Y, Takahashi I *et al*. Temporal and spatial gene expression of major bone extracellular matrix molecules during embryonic mandibular osteogenesis in rats. *Histochem J* 2001; 33:25–35.

51. Hao Y, Yan H, Wang X *et al*. Evaluation of osteoinduction and proliferation on nano-Sr-HAP: a novel orthopedic biomaterial for bone tissue regeneration. *J Nanosci Nanotech* 2012; 12:207–12.